Dynamic chemical devices: Modulation of contraction/extension molecular motion by coupled-ion binding/pH change-induced structural switching

Mihail Barboiu* and Jean-Marie Lehn†

Institut de Science et d'Ingénierie Supramoléculaires, Université Louis Pasteur, Centre National de la Recherche Scientifique/Unité Mixte de Recherche 7006, 4 Rue Blaise Pascal, 67000 Strasbourg, France

Contributed by Jean-Marie Lehn, February 19, 2002

Dynamic chemical devices involve morphological or constitutional modifications in molecular or supramolecular systems, induced by internal or external physical or chemical triggers. Reversible changes in shape result in molecular motions and define motional dynamic devices presenting mechanical-like actions of various types. Suitably designed polyheterocyclic strands such as compounds 1–5 wrap into helical conformations. The binding of lead(II) ions to the coordination subunits contained in the strand leads to complete uncoiling and yields a polymetallic complex presenting a fully extended shape. The addition of a cryptand complexing agent that strongly binds lead(II) ions and releases them under protonation allows a reversible pH-modulation of lead(II) levels in the medium, which in turn induces coiling/uncoiling of the molecular strand. This system thus represents a motional dynamic device which performs a mechano-chemical process, realizing alternating extension/contraction motions triggered by ion binding. It achieves a linear motor-type of action of very large stroke amplitude fueled by ionic processes.

The design of functional chemical devices is a major facet of supramolecular chemistry (1, 2). It is based on the structural organization and functional integration within a molecular or supramolecular architecture of components presenting features such as photo-, electro- or iono-activity.

Chemical systems undergoing dynamic structural changes may be considered to encompass two types of behavior of basically very different nature and a third one that combines the two:

morphological dynamics, comprising molecular or supramolecular entities that undergo reversible shape changes triggered by external stimuli, resulting in *motional* ("mechanical") processes;

constitutional dynamics, concerning molecular or supramolecular entities that undergo reversible changes in constitution by exchange, incorporation, or decorporation of components, generating pools of interconverting species such as occur in dynamic combinatorial chemistry (3, 4);

combined *constitutional/motional* dynamics, where constitutional modifications by exchange, addition, or subtraction of components cause structural changes that result in motional effects by an interplay of self-assembly and deassembly, growth and decay.

We shall consider here motional dynamic devices (5–8). They comprise a wide variety of species susceptible of undergoing structural modifications under the action of stimuli such as light, electron transfer, or ion binding, resulting in photo-, electro-, or iono-active devices, respectively. They define a range of mechanical features presenting "molecular machine" (mechano-device) type character, from the classical, extensively implemented, large shape variations produced by the thermally or photo-driven *cis*-trans isomerization of azobenzene derivatives to the sophisticated rotaxane and catenane entities that allow the relative positioning of mechanically maintained, interlocked components (for reviews, see ref. 6–8). Thus, for instance, rotary (6) and linear (8) motions, triggered by electrochemical reactions, have been realized recently. Of special interest is ionic modulation, i.e., shape changes produced by ion binding, in view of its relation to ion-induced processes in biology.

In our group, we have been interested over the years in a number of spontaneous or triggered dynamic processes such as reorientation of a substrate in a cyclodextrin receptor (9), cation jumps inside a cryptate cavity (10), electrochemical interconversion of double-helical and single-stranded complexes (11) or, more recently, rotational translation in an artificial double helix (12).

Controlled structural modifications play a most important role in biology, where they are key to the functioning of motor proteins such as myosin in muscle action, kinesins, and dyneins (13, 14), of rotary motion in the multiprotein ATP synthase assembly (15, 16, 47), etc. Such dynamic processes are of mechano-chemical nature, involving chemical reactions like ATP/ADP interconversion, proton transfer, or ion binding.

The formation and dissociation of actin filaments and microtubules, as they occur in mitotic and meiotic spindles, represent a type of combined constitutional/motional behavior, which may even propel a complete organism as in the displacement of the bacterium *Listeria* (13, 14).

Contraction-extension motions of helical protein supercoils occur in the bacterial flagellar protofilament (17, 18), but related artificial systems are rare. For instance, chemists have designed entities such as synthetic chains of amino acids (19) or aromatic helical backbones (20), responsive polymers (21, 22), or other species (for a selection, see refs. 23–27), which undergo important shape changes, e.g., folding/unfolding, rotation or linear motions in response to external stimuli (light, temperature, pressure, or medium effects).

We describe herein the ionic modulation of extension/contraction motions in a type of helical coil (**H**)/linear chain (**L**) reversible switching process, triggered by multiple complexation–decomplexation reactions. The corresponding $\mathbf{H} \rightleftharpoons \mathbf{L}$ interconversion is schematically represented in Fig. 1*a*.

Concept: Design of the Components

Molecular self-organization into helical architectures is quite common for biological macromolecules (e.g., polypeptides, double stranded DNA), where various noncovalent interactions contribute to the formation and stabilization of such structures.

CHEMISTRY

Abbreviations: ROESY, rotating-frame Overhauser effect spectroscopy; NOE, nuclear Overhauser effects; eq, equivalents.

*Present address: Institut Européen des Membranes, Centre National de la Recherche Scientifique/Unité Mixte de Recherche 5635, 1919 Route de Mende, F-34293 Montpellier Cedex 5, France.

†To whom reprint requests should be addressed. E-mail: lehn@chimie.u-strasbg.fr.

The publication costs of this article were defrayed in part by page charge payment. This article must therefore be hereby marked "*advertisement*" in accordance with 18 U.S.C. §1734 solely to indicate this fact.

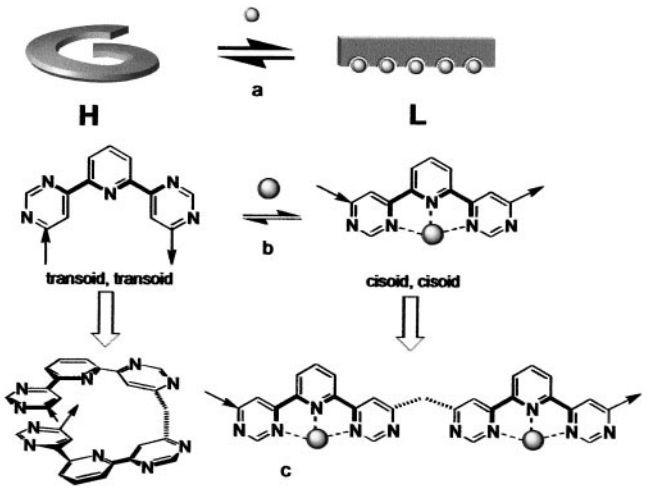

Fig. 1. Concept and design of an ion-triggered molecular dynamic device. (*a*) Ionic modulation of extension/contraction motions interconverting the helical-free ligand **H** and the extended linear multinuclear complex **L**. (*b* and *c*) Preferential *transoid, transoid* conformation leading to helical winding of extended pyridine-pyrimidine sequences (*Left*) and induced *cisoid, cisoid* conformation resulting from tridentate coordination of transition metal ions yielding a linear conformation of the strand (*Right*).

It has recently been shown in our group that oligoheterocyclic strands **1**-**5** consisting of alternating pyridine (py) and pyrimidine (pym) subunits connected in α,α' positions fold into helical superstructures. Thus, the (py-pym) sequence represents a general *helicity codon* inducing molecular self-organization of the strand into helical form. Strands of this type—**2** (28–30), **4** (29, 30) and **5** (ref. 31; Scheme 1)—have indeed been found to adopt one-turn **2**-**H**, two-turn **4**-**H**, and three-turn **5**-**H** helical structures, respectively, in solution and in the solid state. This approach was further developed toward extended oligomers, up to one containing 27 heterocycles, which forms a four-turn helix (31). In view of the strongly favored *transoid* conformation about the connecting NC–CN bond in α,α'-bipyridine (bipy; refs. 32 and 33), α,α'-(py,pym) units are expected to present a similar or even stronger preference for the *transoid* form, so that α,α'-linked, extended (py-pym) sequences strongly enforce helical winding of the strand (28–31).

On the other hand, metal-ion binding imposes the *cisoid* arrangement, as is common in the very numerous complexes of bipy. Thus, for a (pym-py-pym) sequence, tridentate metal ion coordination converts the *transoid*, *transoid* form of the free ligand to the *cisoid*, *cisoid* form, corresponding to a terpyridine (terpy)-type complexation site (Fig. 1*b*). Such is indeed the case for strands **1**, **2**, and a related one (with $n = 4$), where the binding of ions such as Zn(II), Co(II), Ru(II), or Pb(II) yields rack- (34, 35), grid- (36–38), and cage-type (39) coordination architectures.

Specifically, the conversion of a free ligand, composed of a sequence of (py-pym) units, into a polymetallic rack-type complex (34), transforms a helical molecular strand into a rigid linear coordination array (Fig. 1*c*) and results in large-amplitude molecular motion $\mathbf{H} \rightleftharpoons \mathbf{L}$ triggered by metal-ion binding (Fig. 1*a*). Such a process results in the production of mechanical action at the supramolecular level in an iono-mechanical molecular device (1), through controlled extension-contraction motions by interconversion of helically wrapped and linear entities induced by a reversible chemical switching operation using appropriate metal ions. One may consider that it amounts to a nanodevice presenting triggered linear motor-type action.

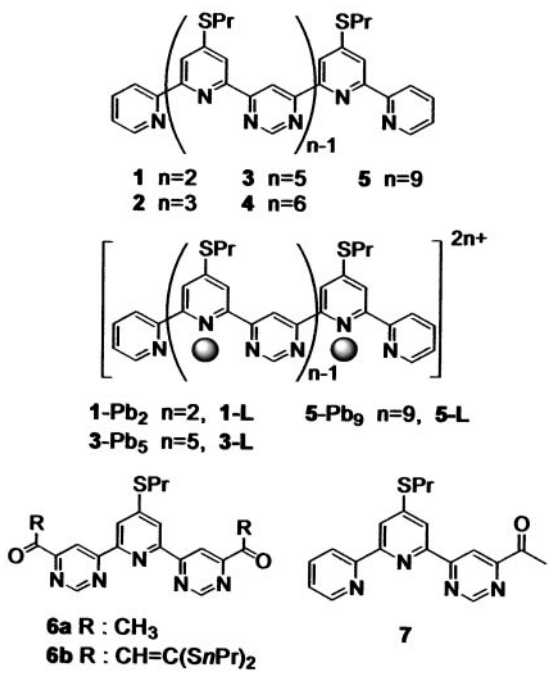

Scheme 1.

Materials and Methods

NMR Spectrometric Measurements. ^{1}H NMR, ^{207}Pb NMR, correlated spectroscopy (COSY), rotating-frame Overhauser effect spectroscopy (ROESY), and ^{1}H-^{207}Pb NMR correlation measurements were recorded on AC 200 and ARX 500 Bruker spectrometers in $CDCl_3$ and CD_3CN, with the use of the residual solvent peak as reference. The heteronuclear ^{1}H-^{207}Pb correlation NMR was done by using an HMQC experiment with *z* gradient selection. MS analysis was performed on a VG BioQ triple-quadrupole mass spectrometer upgraded to obtain Quatro II performance (Micromass, Manchester, U.K.). The microanalyses were carried out at Service de Microanalyses, Institut Charles Sadron, Strasbourg, France.

Synthesis of Compound 3. Strand **3** was synthesized by following procedures developed earlier (30, 31). It will be described in detail elsewhere. Its properties agree with the structure.

Generation of Complex [1-Pb$_2$(OTf)$_4$]. Formation by addition of $Pb(OTf)_2$ (10.62 mg) to ligand **1** (5 mg) in CD_3CN (0.5 ml). $Pb(OTf)_2$ was prepared from PbO and CF_3SO_3H as reported (37). For the structural characterization, see the text. ^{1}H NMR (500 MHz, CD_3CN): $\delta = 10.01$ (s, 2H, H8), 9.21 (s, 2H, H7), 9.05 (d, $J =$ 4.4, 2H, H1), 8.73 (d, $J = 1.3$, 2H, H6), 8.63 (d, $J = 7.6$, 2H, H4), 8.42 (d, $J = 1.3$, 2H, H5), 8.32 (dd, $J = 7.6$, 2H, H3), 7.94 (dd, $J =$ 4.4, 2H, H2), 3.44 (dt, $J = 7.3$, 4H), 1.95 (m, 4H), 1.18 (m, 6H); assignments made on the basis of the COSY and the ROESY spectra; ^{207}Pb NMR (reference $Pb(OTf)_2$, $\delta_{ref} = 6480.7$): $\delta =$ 1652.33 (2), ES-MS: m/z (%): 1994.2 (32) $[(\mathbf{1},Pb_2)(OTf)_3]^+$, 922.6 (40) $[(\mathbf{1},Pb_2)(OTf)_2]^{2+}$, 565.4 (100) $[(\mathbf{1},Pb_2)(OTf)]^{3+}$; $C_{34}H_{66}N_6S_6O_{12}F_{12}Pb_2$ (1,547.8 g/mol).

Generation of Complex [3-Pb$_5$(OTf)$_{10}$]. Formation by addition of $Pb(OTf)_2$ (10.3 mg) to ligand **3** (5 mg) in CD_3CN, (0.5 ml); for structural characterization, see the text. ^{1}H NMR (500 MHz, CD_3CN): $\delta = 10.15$ (s, 2H, H12), 10.08 (s, 2H, H8), 9.36 (s, 2H, H11), 9.30 (s, 2H, H7), 9.07 (d, $J = 4.4$, 2H, H1), 8.90 (s, 2H, H13), 8.89 (d, $J = 1.3$, 2H, H10), 8.88 (d, $J = 1.3$, 2H, H9), 8.78 (d, $J =$ 1.3, 2H, H6), 8.65 (d, $J = 7.6$, 2H, H4), 8.46 (d, $J = 1.3$, 2H, H5), 8.36 (dd, $J = 7.6$, 2H, H3), 7.99 (dd, $J = 4.4$, 2H, H2), 3.55 (dt, $J =$ 7.3, 8H), 3.45 (t, $J = 7.0$, 2H), 1.95 (m, 10H), 1.21 (m, 15H);

assignments made on the basis of the COSY and the ROESY spectra; ^{207}Pb NMR (reference $Pb(OTf)_2$, δ_{ref} = 6480.7): δ = 1653.33 (2), 1143.5 (2), 1139.33 (1); ES-MS: *m/z* (%): 1728 (15) $[(\mathbf{3},Pb_5)(OTf)_8]^{2+}$, 1101.6 (42) $[(\mathbf{3},Pb_5)(OTf)_7]^{3+}$, 799.1 (15) $[(\mathbf{3},Pb_5)(OTf)_6]^{4+}$, 543.9 (30) $[(\mathbf{3},Pb_5)(OTf)_5]^{5+}$, 438.7 (100) $[(\mathbf{3},Pb_5)(OTf)_4]^{6+}$; $C_{76}H_{61}N_{15}S_{15}O_{30}F_{30}Pb_{10}$ (3,750.6 g/mol).

Generation of Complex [5-Pb$_9$(OTf)$_{18}$]. Formation by addition of $Pb(OTf)_2$ (10.6 mg) to ligand **5** (5 mg) in CD_3CN, (0.5 ml); for structural characterization, see the text. ^{1}H NMR (CD_3CN): δ = 10.16 (s, 8H, H8,12,16,20), 9.37 (s, 8H, H7,11,15,19), 9.05 (m, 2H, H4), 8.91 (s, 7H, H17,18,21), 8.89 (s, 5H, H10,13,14), 8.77 (s, 4H, H6,9), 8.65 (m, 2H, H1), 8.46 (m, 2H, H5), 8.38 (m, 2H, H3), 8.05 (m, 2H, H2), 3.58 (t, *J* = 7.3, 4H), 3.24 (t, *J* = 7.0, 14H), 1.95 (m, 18H), 1.21 (m, 18H); assignments made on the basis of the COSY and the ROESY spectra; ^{207}Pb NMR (reference $Pb(OTf)_2$, δ_{ref} = 6480.7): δ = 1650.9 (2), 1141.1 (1), 1134.0 (6); ES-MS: *m/z* (%): $[(\mathbf{4},Pb_9)(OTf)_{14}]^{4+}$, 1523.4 (10), $[(\mathbf{4},Pb_9)(OTf)_{13}]^{5+}$, 1188.9 (11), $[(\mathbf{4},Pb_9)(OTf)_{12}]^{6+}$, 965.9 (40), $[(\mathbf{4},Pb_9)(OTf)_{11}]^{7+}$, 806.62 (100) $[(\mathbf{4},Pb_9)(OTf)_{10}]^{8+}$, 806.62 (100); $C_{132}H_{105}N_{27}S_{27}O_{54}F_{54}Pb_9$ (6,689.9 g/mol).

Crystal Structure Data for Complex [1-Pb$_2$(OTf)$_4$]. Structure determination and structural features will be described elsewhere (A. DeCian, N. Kyritsakas, M.B., and J.-M.L., unpublished work).

Results and Discussion

Synthesis and Structure of Strands 1–5. The ligands **1** and **2** were previously synthesized (29, 30) and used in the self-assembly of metallo-supramolecular [n × n] grid arrays with Pb(II) ions (37). Compound **3** was obtained by using the Potts methodology (40) following processes developed earlier (30, 31): repetitive reaction of a bifunctional central pyrimidine bis-Michael acceptor unit **6b**, prepared from **6a** (31), with two acetyl building blocks **7** (30) gave **3** in 30% yield. Compound **4** (30) and the extended strand **5** (31) have been described earlier.

According to previous work, all strands **1-5** adopt a strongly enforced helical conformation, presenting up to four turns; several such molecular helices have been characterized by X-ray crystallography (28–31). Thus, the ^{1}H NMR spectrum of **3** (see Fig. 5) is consistent with the presence of a helical conformation of the polyheterocyclic strands. As expected, it displays an anisotropic upfield shift for the hydrogens H2 and H3 on the terminal pyridine rings at δ = 6.73 and = 7.08 ppm, respectively. Moreover, distinct nuclear Overhauser effects (NOE) are observed between the protons oriented toward the interior of the helix, e.g., between the H5 protons of the two external pyrimidines and both the H3 protons of the two terminal pyridine groups and the H5 proton of the internal pyrimidine. On the basis of these NMR data, one may conclude that the molecular strand **3** adopts a helical conformation that is expected to present about 1.75 turns.

Metal-Ion Binding and Structure of the Complexes. *Complex [1-Pb(OTf)$_4$].* Rack-type complexes of ligands **1** and **2** with Ru(II) have been described (34, 35). For the purposes of this work, the related complexes with the much larger Pb(II) ions were investigated in view of the lesser pinching of the tridentate terpy-Pb(II) coordination site (37), compared with the corresponding complexes with transition metal ions (34, 35), and with the expected far greater reversibility caused by easier complexation-decomplexation.

Treatment of **1** with 2 equivalents (eq) of $Pb(OTf)_2$ (OTf = triflate, $CF_3SO_3^-$) (37) in acetonitrile afforded a compound whose ^{1}H-NMR and electrospray (ES) mass spectral properties (not shown) agree with the formation of a dinuclear [2]-rack type complex [**1**-Pb_2 $(OTf)_4$]. Confirmation was obtained by determination of its crystal structure by X-ray crystallography. The crystal structure showed the complex to be composed of one ligand, two lead cations coordinating each of two triflate anions, and one acetonitrile bound to one lead cation (Fig. 2). The ligand adopts a linear shape **1**-**L** with *cisoid* conformation around all inter-heterocyclic bonds. The pinching angle provides information about the shape of the complexes (35), smaller values being correlated with an increased linearity of the ligand in the complex. It is much smaller for **1**-Pb_2 (10.1°) than for the analogous Ru(II) complex (25.6°; ref. 35). Thus, the binding of the large lead(II) ions generates a more linear shape, a feature of much interest in the context of this work. The representations of the extended polymetallic racks **3**-Pb_5 and **5**-Pb_9 were modeled on the basis of the present crystal structure of the [2]-rack type complex **1**-**L** (see below).

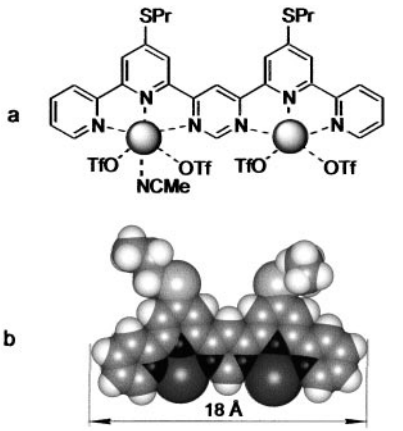

Fig. 2. Representation of the dinuclear Pb(II) rack, **1**-**L**. (*a*) Structure of the complex showing the coordination environment of the Pb(II) cation. (*b*) Space-filling representation of the crystal structure showing only ligand 1 and the two lead(II) cations with indication of the end-to-end length of the ligand in the complex. Solvent molecules included in the crystals are omitted for clarity. Carbon, sulfur, light gray; hydrogen, white; nitrogen, black; lead, gray.

Complex [3-Pb$_5$(OTf)$_{10}$]. A mixture of ligand **3** and 5 eq $Pb(OTf)_2$ in acetonitrile was stirred overnight at room temperature. The ^{1}H NMR spectrum of the resulting complex indicated a high symmetry, consistent with the [5]-rack complex [**3**-$Pb_5(OTf)_{10}$]. The linear conformation is clearly indicated by the ROESY spectrum which shows distinct NOE effects between the terminal pyridine H5 and the neighboring SPr-pyridine H3 protons, as well as between the H5 protons of the pyrimidines and the nearby H3 protons of the neighboring two SPr-pyridines (not shown). The ^{207}Pb NMR spectrum displayed three signals in a 1:2:2 ratio, corresponding to Pb(II) cations in three different chemical environments (Fig. 3*a*). On the basis of the 2D ^{207}Pb-^{1}H correlation spectrum (not shown), the lead signals from right to left may be assigned as follows [$Pb_{position}$ (number of vicinal Pb ions, type and number of nitrogen sites)]: $Pb_{central}$ (2, Py, Pym_2), $Pb_{interior}$ (2, Py, Pym_2), and $Pb_{terminal}$ (1, Py_2, Pym). Thus, the strong NOE effects, the chemical shifts and relative intensity of ^{207}Pb signals, as well as the 2D Pb-proton correlations agree with the linear [5]-rack structure **3**-**L** of the complex (Fig. 4*a*). Furthermore, the ES mass spectrum of this complex showed peaks corresponding to multiply charged species with the correct composition [**3**-$Pb_5(OTf)_n]^{10-n}$, with n = 4–8 (see *Materials and Methods*).

Complex [5-Pb$_9$(OTf)$_{18}$]. A mixture of ligand **5** and 9 eq of $Pb(OTf)_2$ in acetonitrile was stirred overnight at room temperature. The ^{1}H NMR spectrum of the resulting complex indicated high symmetry, which is consistent with complex [**5**-$Pb_9(OTf)_{18}$]. The linear conformation of the ligand in the complex is clearly indicated in the ROESY spectrum; distinct NOE effects are observed between the terminal pyridine H5 and the vicinal SPr-pyridine H3 protons as well as between the H5 pyrimidine protons and the nearby H3 protons of the neighboring two SPr-pyridines. The ^{207}Pb NMR spectrum shows three signals in a 2:1:6 ratio, corresponding

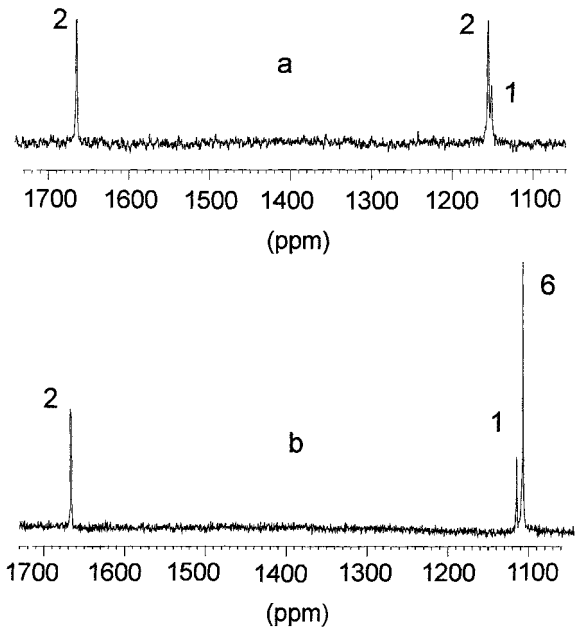

Fig. 3. 83 MHz ^{207}Pb NMR spectra of complexes [**3**-$Pb_5(OTf)_{10}$] and [**5**-$Pb_9(OTf)_{18}$] in CD_3CN at 25°C.

to Pb(II) cations in three different chemical environments (Fig. 3*b*). On the basis of the 2D ^{207}Pb-^{1}H correlation spectrum, the lead signals at 1,134.0 ppm (intensity 6), 1,141.1 ppm (intensity 1), and 1,650.9 (intensity 2) may be assigned as follows [$Pb_{position}$ (number of vicinal Pb ions, type and number of nitrogen sites)]: $Pb_{interior}$ (2, Py, Pym_2), $Pb_{central}$ (2, Py, Pym_2), and $Pb_{terminal}$ (1, Py_2, Pym). Again, the strong NOE effects, the chemical shifts and relative intensity of the ^{207}Pb signals, as well as the 2D Pb-proton correlations agree with a linear [9]-rack structure **5-L** of the complex (Fig. 4*b*). In addition, the ES mass spectrum of this complex showed peaks that correspond to multiply charged species possessing the correct composition [**5**-$Pb_9(OTf)_n]^{18-n}$, with n = 12–16 (see *Materials and Methods*).

Structural features of the complexes. The radiocrystallographic and spectroscopic data indicate that all three complexes—**1**-Pb_2, **3**-Pb_5, and **5**-Pb_9—present a rack-type structure. Binding of the Pb(II) ions by imposing terpy-type coordination sites, converts all *transoid* inter-heterocyclic connections in the ligands into *cisoid* connections (Fig. 1*b*). It results in a linearization of the ligand from the helical strands **1-H**, **3-H**, and **5-H** into the extended unfolded forms present in the complexes **1-L**, **3-L**, and **5-L** (Figs. 2 and 4).

Modelization of the structures of these complexes on the basis of the geometry of **1-L** in the crystal structure of [**1**-$Pb_2(OTf)_4$] obtained above (Fig. 2), yields curved extended entities of about 38-Å and 60-Å lengths for **3-L** and **5-L**, as represented in Fig. 4. Whereas the helical free ligands **H** may be expected to behave like

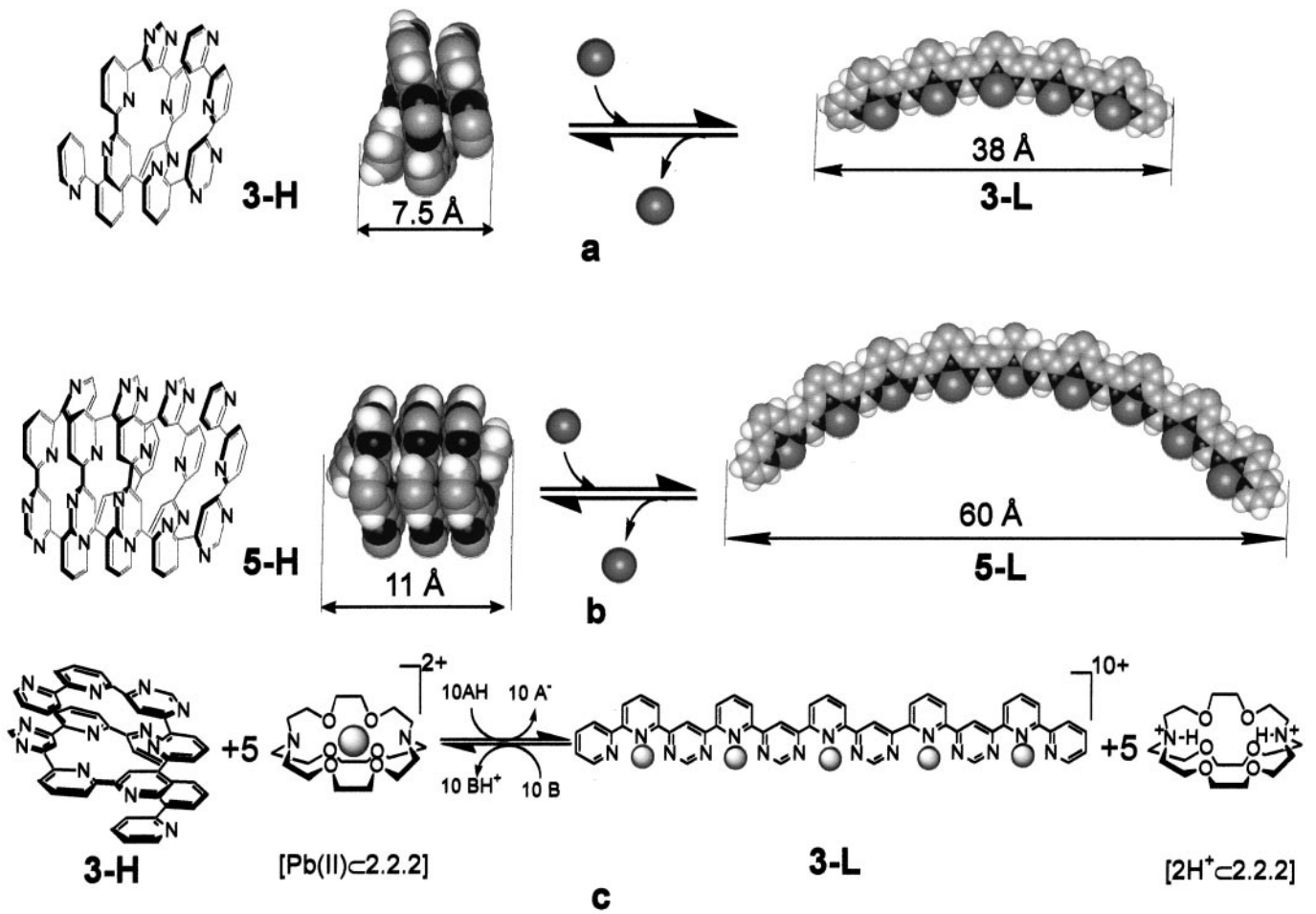

Fig. 4. (*a* and *b*) Modelization of the extended rack-type complexes **3-L** (*a*) and **5-L** (*b*) on the basis of the crystal structure of complex **1-L** (Fig. 2) with indication of the end-to-end length of the ligand in the complexes. (*c*) Acid-base processes modulating coiling/uncoiling motions by interconversion of the helical strand **3-H** and the extended linear complex **3-L**. The gray spherical objects represent Pb(II) ions; AH═CF_3SO_3H, B═Et_3N. The S*n*Pr substituents on the ligands have been omitted for clarity.

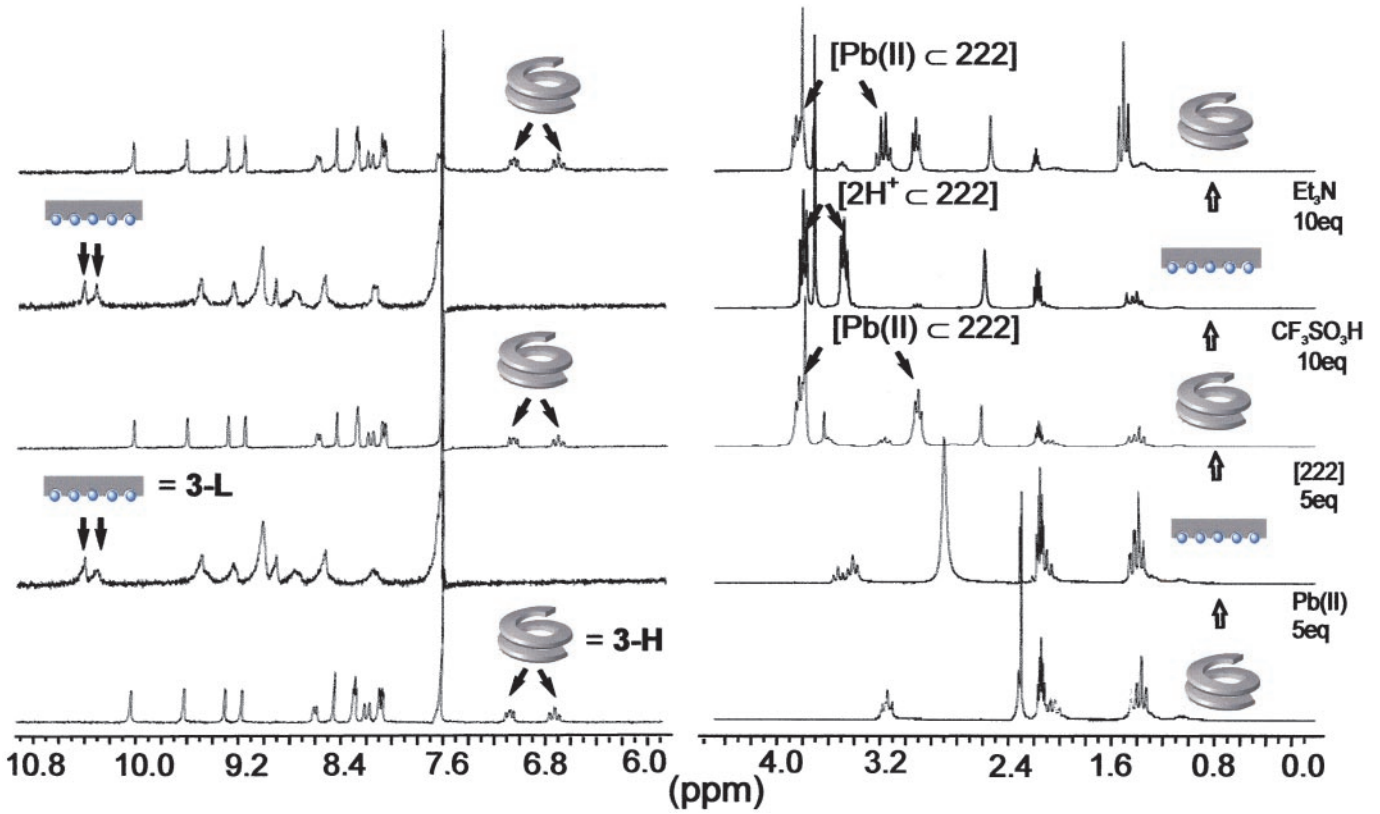

Fig. 5. 400 MHz ^{1}H spectral changes on structural interconversion in the system [**3**, 5 eq $Pb(OTf)_2$,[2.2.2], CF_3CO_2H, Et_3N] on successive addition of the different triggering reagents, in $CDCl_3/CD_3CN$ 2/1 solution (see text). The arrows indicate signals characteristic of the species shown. The aromatic domain (*Left*) of the spectra is amplified by a factor of four with respect to the aliphatic region (*Right*).

a molecular spring, the corresponding complex **L** should be a rigid, bent molecular stick.

Ionic modulation of extension/contraction molecular motion. The transformation of the helical-free ligands **1-H**, **3-H**, and **5-H** into the corresponding rigid linear complexes **1-L**, **3-L**, and **5-L** by the binding of several Pb(II) ions offers the unique opportunity to set up a reversible motional process in which a molecular entity undergoes sequential extension and contraction phases triggered by external chemical signals. Stretching/contracting actions occur in the folding/unfolding of proteins (41, 42).

A system allowing to produce reversible pulses of Pb(II) ions was achieved by taking advantage of the properties of the macrobicyclic ligand, cryptand [2.2.2] (43), which forms cryptate inclusion complexes $[M^{n+}\subset 2.2.2]$ with numerous metal ions (43, 44). In particular Pb(II) yields a very stable cryptate [Pb(II)⊂2.2.2] (Scheme 1*c*), with stability constants log K_s of about 12.5 and 12.9 in aqueous solution (44, 45) and in CH_3OH (46) respectively. Even higher stability may be expected in the $CDCl_3/CD_3CN$ 2/1 solvent used here (see below). Furthermore, protonation of the bridgehead nitrogen sites leads to the deprotonated species $[2H^+\subset 2.2.2]$ (Fig. 4*c*) with release of the included Pb(II) cation from the cryptate (44).

Thus, one may consider to set up a multicomponent/multitrigger system involving a helical ligand strand **1-5**, Pb(II) ions, cryptand [2.2.2], acid, and base. Such a system should undergo the following reactions:

complexation: $\mathbf{H} + n\ Pb(II) \rightarrow \mathbf{L}$.
cryptate formation: $\mathbf{L} + n[2.2.2] \rightarrow \mathbf{H} + n[Pb(II)\subset 2.2.2]$
ion release from cryptate by protonation: $[Pb(II)\subset 2.2.2] + 2H^+ \rightarrow [2H^+\subset 2.2.2] + Pb(II)$
deprotonation: $[2H^+\subset 2.2.2] + 2(Base) \rightarrow [2.2.2] + 2(Base, H^+)$

As a result, sequential protonation/deprotonation should lead to alternate [Pb(II) release]/[Pb(II) cryptation] and thus to $\mathbf{L} \rightleftharpoons \mathbf{H}$ interconversion. That this is indeed the case is clearly indicated by the changes occurring in the proton NMR spectrum of the system. Fig. 5 shows the evolution of the aromatic and aliphatic part of the ^{1}H NMR spectra as a function of the triggering agent, for the system involving ligand **3**, Pb(II), [2.2.2], CF_3SO_3H, and Et_3N.

The addition of 5 eq of $Pb(OTf)_2$ to a solution [$CDCl_3/CD_3CN$ = 2/1 (vol/vol)] of helical ligand **3-H** leads to the linear [5]-rack **3-L**. This transformation is characterized by the disappearance of the signals of the terminal pyridine hydrogens H2 and H3 (at 6.73 and

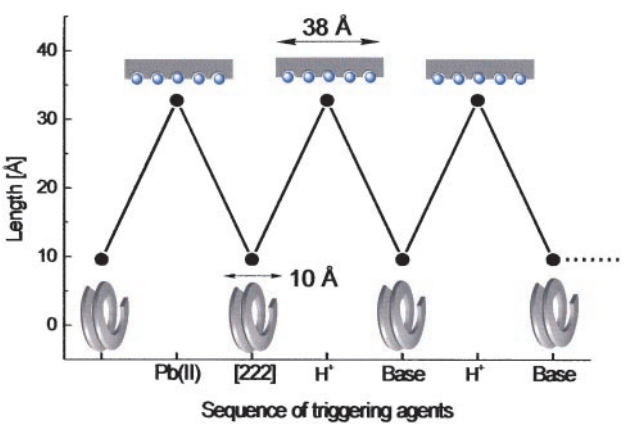

Fig. 6. Modulation of the coiling/uncoiling, contraction/extension process **3-H** $\rightleftharpoons$ **3-L** by coupled-ion/pH-induced structural switching.

7.08 ppm) and by the appearance of the signals of the Pb(II) complexed-pyrimidine hydrogens H8 and H12 (at 10.31 and 10.43 ppm). On addition of 5 eq of the strong Pb(II) complexing agent, the [2.2.2] cryptand, the spectrum of the helical form **3-H** is restored, and the aliphatic part of the spectrum shows peaks that correspond to the cryptate complex [Pb(II)⊂2.2.2]. Subsequent addition of 10 eq of CF_3SO_3H induces protonation of the [2.2.2] nitrogen sites, thus releasing the Pb(II) ions, which then complex the helical form **3-H**, regenerating the linear **3-L**. The aliphatic part of the spectrum displays the peaks characteristic of the protonated cryptate [$2H^+$⊂2.2.2]. Deprotonation of the latter by addition of Et_3N results in the reformation of the cryptate [Pb(II)⊂2.2.2] and of helical **3-H**. Alternating contraction/extension motions between the helical strand **3-H** and the linear [5]-rack **3-L** thus may be repetitively triggered by successive additions of acid and base, leading to the sequential exchange of Pb(II) between the ligand **3** and the [2.2.2] cryptand.

These data demonstrate the modulation of a coiling/uncoiling process by a coupled-ion/pH-induced structural switching. Thus, extension/contraction is realized as a controlled motion in an oscillatory periodic sequence (Fig. 6). It amounts to a two-stroke, linear motor-type action with a very large stroke amplitude from 7.5 Å to 38 Å, and from 11 Å to 60 Å in the case of strands **3** and **5,** respectively (Fig. 4). This mechano-chemical process is fueled by protonation/deprotonation i.e., by acid/base neutralization energy.

Conclusion

Although of long standing, the field of molecules undergoing movements triggered by external agents (for instance by light) has received increased attention during recent years, in particular with the hope of mimicking the molecular motions of highly complicated biological systems (6–8). Circular motions (6) and linear extension/contraction processes (8) have been induced by chemical reactions. The present results show that, by using a rationally designed helical molecular strand and a simple chemical mechanism, it becomes possible to control a coiling-uncoiling motion[‡] by chemical reactions in a manner reminiscent of that of proteins capable of transforming chemical modifications into motion (13, 14). Oscillatory shape changes have been identified in protein folding/unfolding processes (41, 42). Attaching molecules such as those studied here to a surface may be expected to generate oriented linear motions capable of producing expansion/contraction on the nanometric scale.

The system described here represents a prototype for a molecular actuator/engine type of dynamic device "fueled" by ionic processes. On the other hand, such ionically triggered shape changes also amount to coupling and transduction between structural and ionic signals, a feature of much interest for supramolecular information transfer.

[‡]It is reminiscent of the coiling/uncoiling motion of the tail of a rather unique but widely known animal, the "marsupilami" [Franquin, A., Batem & Greg (1987) *La Queue du Marsupilami* (Marsu Productions, Monaco)].

We thank N. Kyritsakas and Dr. A. de Cian (Laboratoire de Cristallochimie, Université Louis Pasteur, Strasbourg) for the crystal structure studies on complex [**1**-$Pb_2(OTf)_2$], Dr. R. Graff for NMR measurements, and Dr. H. Nierengarten for electrospray mass spectrometric measurements. The sample of compound **5** was available from earlier work by Dr. M. Ohkita. This research was supported by a Collège de France postdoctoral fellowship (to M.B.).

1. Lehn, J.-M. (1995) *Supramolecular Chemistry-Concepts and Perspectives* (VCH, Weinheim, Germany), 89–138.
2. Steed, J. W. & Atwood, J. L. (2000) in *Supramolecular Chemistry* (Wiley, Chichester, U.K.), pp. 573–640.
3. Lehn, J.-M. (1999) *Chem. Eur. J.* **5,** 2455–2463.
4. Cousins, G. R. L., Pulsen, S. A. & Sanders, J. K. M. (2000) *Curr. Opin. Chem. Biol.* **4,** 270.
5. Lehn, J.-M. (1999) *Supramolecular Science: Where It Is and Where It Is Going*, eds. Ungaro, R. & Dalcanale, E. (Kluwer, Dordrecht, The Netherlands), pp. 287–304.
6. Balzani, V, Credi, F., Raymo, M. & Stoddart, J. F. (2000) *Angew. Chem. Int. Ed. Engl.* **39,** 3348–3391.
7. Stoddard, J. F., ed. (2001) *Acc. Chem. Res.* **34,** 409–522.
8. Collin, J. P., Dietrich-Buchecker, C., Gavina, P., Jimenez-Molero, M. C. & Sauvage, J.-P. (2001) *Acc. Chem. Res.* **34,** 477–487.
9. Behr, J.-P. & Lehn, J.-M. (1976) *J. Am. Chem. Soc.* **98,** 1743.
10. Lehn, J.-M. & Stubbs, M. E. (1974) *J. Am. Chem. Soc.* **96,** 4011.
11. Gisselbrecht, J.-P., Gross, M., Lehn, J.-M., Sauvage, J.-P., Ziessel, R., Piccinni-Leopardi, C., Arrieta, J.-M., Germain, G. & Van Meerssche, M. (1984) *Nouv. J. Chim.* **8,** 661.
12. Berl, V., Huc, I., Khoury, R. G., Krische, M. J. & Lehn, J.-M. (2000) *Nature (London)* **40,** 7720–7723.
13. Alberts, B., Bray, D., Lewis, J., Raff, M., Roberts, K. & Watson, J. D. (1994) in *Molecular Biology of the Cell* (Garland, New York), 3rd Ed., pp. 786–861.
14. Kreis, T. & Vale, R., eds. (1999) *Cytoskeletal and Motor Proteins* (Oxford Univ. Press, Oxford), 2nd Ed.
15. Boyer, P. D. (1998) *Angew. Chem. Int. Ed. Engl.* **37,** 2296–2307.
16. Allison, W. S. (1998) *Acc. Chem. Res.* **31,** 819–826.
17. Namba, K. & Vonderviszt, F. (1997) *Q. Rev. Biophys.* **30,** 1–65.
18. Samatey, F. A., Imada, K., Nagashima, S. Vonderviszt, F., Kumasaka, T., Yamamoto, M. & Namba, K. (2001) *Nature (London)* **410,** 331–337.
19. Urry, D. A. (1993) *Angew. Chem. Int. Ed. Engl.* **32,** 819–841.
20. Nelson, J. C., Saven, J. G., Moore, J. S. & Wolynes, P. G. (1997) *Science* **277,** 1793–1796.
21. Osada, Y. & Gong, J. (1993) *Prog. Polym. Sci.* **18,** 187–226.
22. Lendlein, A., Schmidt, A. M. & Langer, R. (2001) *Proc. Natl. Acad. Sci. USA* **98,** 842–847.
23. Rasmussen, P. H., Ramanujam, P. S., Hvilsted, S. & Berg, R. H. (1999) *J. Am. Chem. Soc.* **121,** 4738–4743.
24. Jung, O.-S., Kim, Y. J., Lee, Y.-A., Park, J. K. & Chae, H. K. (2000) *J. Am. Chem. Soc.* **122,** 9921–9925.
25. Bencini, A., Bianchi, A., Lodeiro, C., Masotti, A., Parola, A. J., Pina, F., Seixas de Melo, J. & Valtancoli, B. (2000) *Chem. Commun*., 1639–1640.
26. Corbin, P. S. & Zimmermann, S. C. (2000) *J. Am. Chem. Soc.* **122,** 3779–3780.
27. Yashima, E., Maeda, K. & Sato, O. (2001) *J. Am. Chem. Soc.* **123,** 8159–8160.
28. Hanan, G. S., Schubert, U. S., Volkmer, D. Rivière, E., Lehn, J.-M., Kyritsakas, N. & Fischer, J. (1997) *Can J. Chem.* **75,** 169–182.
29. Bassani, D. M., Lehn, J.-M., Baum, G. & Fenske, D. (1997) *Angew. Chem. Int. Ed. Engl.* **36,** 1845–1847.
30. Bassani, D. M. & Lehn, J.-M. (1997) *Bull. Soc. Chim. Fr.* **134,** 897–906.
31. Ohkita, M., Lehn, J.-M., Baum, G. & Fenske, D. (1999) *Chem. Eur. J.* **12,** 3471–3481.
32. Howard, S. T. (1996) *J. Am. Chem. Soc.* **118,** 10269–10274.
33. Göller, A. & Grummt, U.-W. (2000) *Chem. Phys. Lett.* **321,** 399–405.
34. Hanan, G. S., Arana, C. R., Lehn, J.-M. & Fenske, D. (1995) *Angew. Chem. Int. Ed. Engl.* **34,** 1122–1124.
35. Hanan, G. S., Arana, C. R., Lehn, J.-M., Baum, G. & Fenske, D. (1996) *Chem. Eur. J.* **2,** 1292–1302.
36. Hanan, G. S., Volkmer, D., Schubert, U. S., Lehn, J.-M., Baum, G. & Fenske, D. (1997) *Angew. Chem. Int. Ed. Engl.* **36,** 1842–1844.
37. Garcia, A. M., Romero-Salguero, F. J., Bassani, D. M., Lehn, J.-M., Baum, G. & Fenske, D. (1999) *Chem. Eur. J.* **6,** 1803–1808.
38. Rojo, J., Romero-Salguero, F. J., Lehn, J.-M., Baum, G. & Fenske, D. (1999) *Eur. J. Inorg. Chem.* 1421–1428.
39. Garcia, A. M., Bassani, D. M., Lehn, J.-M., Baum, G. & Fenske, D. (1999) *Chem. Eur. J.* **5,** 1234–1238.
40. Potts, K. T., Gheysen-Raiford, K. A. & Keshavarz-K, M. (1993) *J. Am. Chem. Soc.* **115,** 2793–2807.
41. Winkler, J. R. & Gray, H. B., eds. (1998) *Acc. Chem. Res.* **31,** 697–780.
42. Mayor, U., Johnson, C. M., Daggett, V. & Fersht, A. R. (2000) *Proc. Natl. Acad. Sci. USA* **97,** 13518–13522.
43. Lehn, J.-M. (1973) *Struct. Bonding (Berlin)* **16,** 1–69.
44. Lehn, J.-M. & Sauvage, J.-P. (1975) *J. Am. Chem. Soc.* **97,** 6700–6707.
45. Buschmann, H.-J., Cleve, E. & Schollmeyer, E. (1997) *J. Coord. Chem.* **42,** 127–130.
46. Buschmann, H.-J. (1985) *Chem. Ber.* **118,** 3408–3412.
47. Walker, J. E. (1998) *Angew. Chem. Int. Ed*. **37,** 2308–2319.